Analog Beamforming using Time-Modulated Arrays with Digitally Preprocessed Rectangular Sequences

Roberto Maneiro-Catoira, *Member, IEEE,* Julio Brégains, *Senior Member, IEEE,*
José A. García-Naya, *Member, IEEE,* and Luis Castedo, *Senior Member, IEEE*

***Abstract*—Conventional time-modulated arrays are based on the application of variable-width periodical rectangular pulses (easily implemented with radio frequency switches) to the individual antenna excitations. However, a serious bottleneck arises when the number of exploited harmonic beams increases. In this context, the modest windowing features of the rectangular pulses produce an inflexible and ineffective harmonic beamforming. The use of other pulses like sum of weighted cosines partially solves these issues at the expense of introducing additional non-timing variables. We propose the discrete-time preprocessing of rectangular pulses before being applied to the antenna to accomplish an agile, efficient and accurate harmonic beamforming, while keeping the simplicity of the hardware structure.**

***Index Terms*—Time-Modulated Arrays, Beamforming.**

I. Introduction

THE design of Beamforrming (BF) architectures for advanced multi-antenna systems is unavoidably constrained by the trade-off between flexibility, performance and simplicity. In this respect, full-blown digital BF –which requires one Radio Frequency (RF) chain per antenna– uses discrete baseband processing to synthesize the BF weights, offering unbeatable flexibility and performance at the expense of increased complexity, cost and power consumption. Accordingly, digital BF is attractive when the performance outweighs mobility but it becomes unpractical for large-scale antenna systems where the physical space is a handicap.

Alternatively, analog BF is a simple and cost-effective method for generating high-gain pencil beam patterns (especially helpful to mitigate the enormous path losses at high frequencies) but is subject to a series of restrictions in terms of flexibility. Indeed, analog BF is based on a simple hardware scheme: an antenna array whose individual elements are connected via phase shifters and Variable Gain Amplifiers (VGAs) (usually supporting digital control) to a single RF chain, as shown in Fig. 1 for the case of a receive analog beamformer. Nevertheless, its performance is limited by a number of constraints: (1) the use of quantized phase shifts jeopardizes an accurate steering of the beams and/or the nulls; and, conversely, the higher the resolution, the higher the power consumption; (2) phase shifters –especially the passive ones at high frequencies– introduce large insertion losses; and (3) a single beamformer (Fig. 1) only supports a single-stream reception. Therefore, an L-stream fully analog BF receiver using an array of N elements requires L RF front-ends and a Linear Beamforming Network (LBFN) with $L \times N$ phase shifters [1]. Usually, $N \gg L$ (especially with large-scale antennas) and the resulting hardware scheme for this analog BF is still simpler than the digital one.

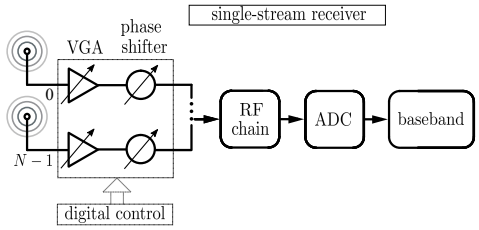

Fig. 1. Receive analog beamformer consisting of a linear array with N isotropic elements, implemented using a network of digitally controlled phase shifters and VGAs.This hardware scheme is not suitable for multi-stream nor multi-user communications.

With the previous pros and cons in mind, hybrid beamforming architectures benefit from the advantages of both analog (generating sharp beams with a simpler hardware) and digital (providing flexibility and performance) domains. In this context, the analog BF will continue to play an increasingly important role. This letter aims to deepen the aforementioned threefold trade-off but focusing on a particular analog BF method, namely the Time-Modulated Array (TMA) BF.

Two different TMA implementation structures have been proposed as alternatives to the one in Fig. 1: 1) conventional TMAs with RF switches [1], [2] (see Fig. 2(a)), in which rectangular pulses become a serious bottleneck in terms of flexibility and efficiency, specially when the number of exploited harmonic beams increases; and 2) the so-called Enhanced TMAs proposed in [3] (see Fig. 2(c)), based on VGAs governed by Sum of Weighted Cosines (SWC) pulses, which solve completely the flexibility problem, but only partially the efficiency issues caused by specular beams corresponding to the negative harmonics and a fundamental mode beam with scanning inability. In this letter we propose a novel TMA structure that overcomes those flexibility and efficiency issues.

II. TMA Beamforming: Strengths and Weaknesses

By replacing the phase shifters and the VGAs in the scheme in Fig. 1 with digitally controlled RF switches –and hence considering a unitary and uniform static distribution of the array excitations– we obtain the conventional TMA

This work has been funded by the Xunta de Galicia (ED431C 2016-045, ED341D R2016/012, ED431G/01), the Agencia Estatal de Investigación of Spain (TEC2013-47141-C4-1-R, TEC2015-69648-REDC, TEC2016-75067-C4-1-R) and ERDF funds of the EU (AEI/FEDER, UE).

The authors are with the University of A Coruña, Spain. E-mail: {roberto.maneiro, julio.bregains, jagarcia, luis}@udc.es

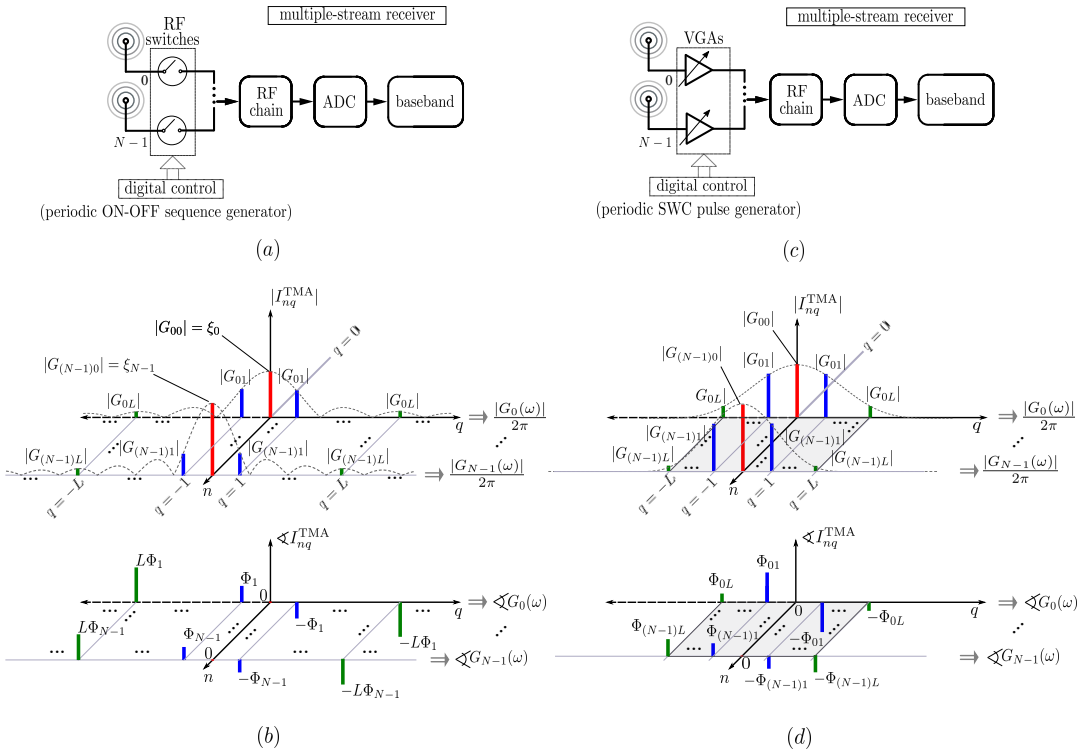

Fig. 2. (a) Multi-stream receiver based on BF with a conventional TMA. (b) Amplitude and phase representation of the dynamic excitations of the TMA in Fig. 2(a). The plot reveals: (1) a modest harmonic windowing behavior when $L > 1$, (2) the presence of duplicated-specular radiation diagrams due to the negative harmonics with same amplitude and opposite phase, (3) the scanning inability for the $q = 0$ beam due to the zero phases, (4) the time-linear control of the amplitudes at $q = 0$ where $\xi_n = \tau_n/T_0$, (5) the proportionality between the phases of harmonics with different order. (c) Multi-stream receiver based on a TMA BF with SWC pulses [3]. (d) Amplitude and phase representation of the dynamic excitations of the TMA in Fig. 2(c).

receiver shown in Fig. 2(a). The application of periodical (T_0) rectangular pulses $g_n(t)$ –easily adjustable in width (τ_n) and delay (δ_n) [2]– to the individual antenna excitations causes the appearance of radiation patterns at the harmonic frequencies $\omega_q = \omega_c + q\omega_0$, with $q \in \mathbb{Z} \setminus \{0\}$, $\omega_0 = 2\pi/T_0$, and ω_c being the carrier frequency. Accordingly, the BF can be performed over the harmonic frequencies ω_q with $q \in \{\pm 1, \pm 2, \cdots, \pm L\}$, where L is the order of the highest exploited harmonic. The array factor –with the term $\mathrm{e}^{j\omega_q t}$ explicitly included– corresponding to the harmonic frequency ω_q is given by $F_q^{\mathrm{TMA}}(\theta, t) = \mathrm{e}^{j\omega_q t} \sum_{n=0}^{N-1} I_{nq}^{\mathrm{TMA}} \mathrm{e}^{jkz_n \cos\theta}$ [1], where z_n represents the n-th array element position on the z axis, θ is the angle with respect to the main axis of the array, k is the wavenumber, and I_{nq}^{TMA} is the complex-valued representation of the per-antenna time-modulated current excitation.

Provided that $\omega_0 > B$ (B is the signal bandwidth), and that the working harmonic patterns are designed (by suitably selecting τ_n and δ_n) fulfilling spatial orthogonality, the first L positive harmonics can be exploited to receive L different incoming signals at ω_c [1]. Such signals are received over different TMA harmonic beams and inherently translated into the corresponding ω_q, occupying a total bandwidth of $L\omega_0$. This multi-stream receiver can be implemented with the extraordinarily simple hardware scheme in Fig. 2(a), with the remarkable benefit of needing a single RF front-end (with a higher bandwidth and a faster Analog to Digital Converter (ADC) than that in Fig. 1). However, such a multi-stream capacity is severely limited. In order to make more visible these constraints, let us firstly consider the following property of the dynamic excitations which is crucial for the harmonic BF design: $I_{nq}^{\mathrm{TMA}} = G_{nq} = G_n(q\omega_0)/2\pi$, with G_{nq} being the Fourier series coefficients of $g_n(t)$, and $G_n(\omega)$ its Fourier transform. $G_n(\omega)$ is a discrete spectrum with impulses at integer multiples of ω_0 and whose envelope is the Fourier transform of the aperiodic basic pulse that conforms a single period of $g_n(t)$.

Accordingly, we can represent both the amplitude and the phase of I_{nq}^{TMA} (functions of τ_n and/or δ_n) in a two-dimensional grid with the variables n and q. Such a portrayal of the TMA for the case of the receiver in Fig. 2(a) is illustrated in Fig. 2(b) and reveals a series of critical aspects that directly impact on the BF performance. Thus, with respect to the TMA power efficiency, and due to the poor windowing features of the sinc envelope[1] of $|I_{nq}^{\mathrm{TMA}}|$, the spectral energy is not efficiently distributed among the working harmonics, causing that, for values of $L > 1$, the antenna efficiency be significantly deteriorated [1]. Moreover, as $g_n(t)$ is a real-valued signal, its Fourier coefficients verify $G_{nq} = G_{n(-q)}^*$, leading to $|F_q^{\mathrm{TMA}}(\theta)|^2 = |F_{-q}^{\mathrm{TMA}}(180° - \theta)|^2$, thus synthesizing a pair of diagrams for q and $-q$, which are symmetric with respect to $\theta = 90°$. In general, such specular "$-q$" diagrams are not useful, spoiling the TMA efficiency even more. This weakness motivated the work in [4], in which a Single-

[1]More specifically, it shows a modest maximum side lobe level of -13 dB and a first order asymptotic decay.

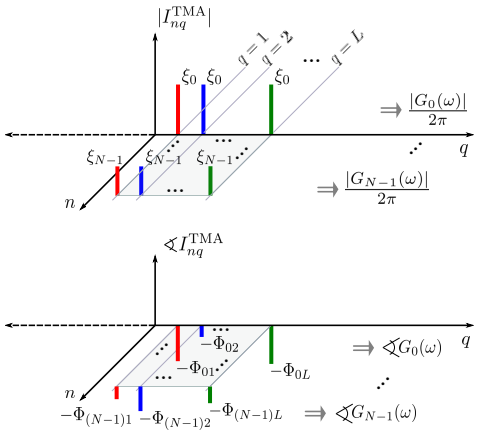

Fig. 3. Amplitude and phase representation of the dynamic excitations of the proposed SSB TMA beamformer.

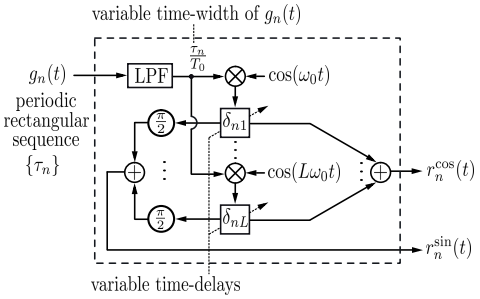

Fig. 4. Block diagram of the preprocessing of the periodic rectangular pulse to synthesize the two quadrature periodic pulses which govern the n-th antenna element of the proposed SSB TMA in Fig. 5.

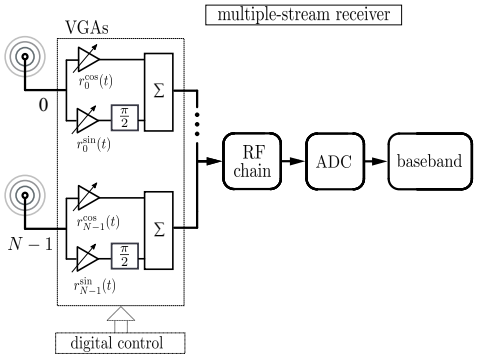

Fig. 5. Proposed multi-stream receiver based on BF with an SSB TMA with preprocessed rectangular sequences.

Sideband (SSB) TMA is modeled with exclusive control over the phase (and hence without Side-Lobe Level (SLL) control) and capable of handling a single beam ($L = 1$).

The second critical aspect in the BF design is the TMA beam-steering efficiency. Remarkably, the efficiency term is not related to the angular accuracy (precisely an advantage of the TMAs which allows for a continuous-time phase control), but to the ability to point each harmonic beam towards the corresponding desired direction. In this regard, we could also include the aforementioned specular "$-q$" beams, which point towards spatial directions probably not usable, but there are other relevant hindrances (see Fig. 2(b)): 1) the scanning inability of the TMA fundamental pattern ($q = 0$) due to the unavoidable zero phases of its excitations ($\sphericalangle I_{n0}^{\text{TMA}} = 0$), and 2) the proportionality between the phases of harmonics of different order, quantitatively, $\Phi_{nq} = -q\Phi_{n1}$, which implies a lack of flexibility to independently steer harmonic beams with different order when $L > 1$.

The TMA beamformer in Fig. 2(c), employs digitally controlled VGAs governed by SWC pulses instead of RF switches [3]. Such a scheme solves the efficiency problem with regard to an appropriate windowing of the working harmonics (see Fig. 2(d)) at the expense of introducing non-timing parameters, but still suffers from the presence of the negative harmonic patterns. Remarkably, the system accomplishes full independence between harmonic beams with different orders thanks to the synthesis of independent dynamic excitation phases $\sphericalangle I_{nq}^{\text{TMA}}$ (see Fig. 2(d)) through the periodic convolution with an auxiliary periodic signal [3].

III. TMA Beamforming Design

In order to solve the BF pending issues detailed above, we propose to address the TMA design taking a desired distribution of the dynamic excitations I_{nq}^{TMA} as a departure point. In this respect, and as a first approach, our aim is to synthesize N identical-in-shape pencil beams (reconfigurable in terms of SLL) with fully-independent steering capacity. Thus, we consider the I_{nq}^{TMA} distribution in Fig. 3. Such a distribution constitutes a bidimensional frequency comb located exclusively in the positive[2] harmonics with the aim of synthesizing a multi-stream receiver based on a SSB TMA. We also highlight the time-linear control of the amplitudes, i.e., $|I_{nq}^{\text{TMA}}| = \tau_n/T_0 = \xi_n$, implying a simpler reconfiguration and a more accurate control of the BF. Regarding $\sphericalangle I_{nq}^{\text{TMA}}$, notice that they are independent as in Fig. 2(d).

Once fixed the desired dynamic excitations, we must design the periodic pulses (governed exclusively by time parameters) as well as the TMA structure capable of synthesizing such time-controlled excitations. The idea is as simple as effective: to filter out the Direct Current (DC) component of each periodic rectangular pulse $g_n(t)$ –corresponding to $G_{n0} = I_{n0}^{\text{TMA}} = \xi_n$– which is the one with a time-linear controlled amplitude, and immediately afterwards, apply a multicarrier complex modulation to such a DC signal (see Fig. 4) in order to shift both time-linear control of the amplitudes[3] and time control of the phases to the spectral lines at the frequencies $q\omega_0$. In Fig. 4, δ_{nq} are time delays[4] that introduce a phase shift in the corresponding dynamic excitation given by $\sphericalangle I_{nq}^{\text{TMA}} = -\Phi_{nq} = -q\omega_0\delta_{nq}$. The quadrature periodic pulses obtained by this procedure allow for implementing the SSB features of the TMA, and are respectively given by (see Fig. 4): $r_n^{\cos}(t) = \xi_n \sum_{q=1}^{L} \cos(q\omega_o t - \Phi_{nq})$ and

[2]Note that the dynamic excitations lines at $q = 0$ are also removed.

[3]Other research lines, out of the scope of TMA philosophy, propose that the amplitude tapering of the pulses be non-timing parameters [5].

[4]Time delays can be accurately implemented in the digital domain through Variable Fractional Delay Filters (VFDFs) [6].

$r_n^{\sin}(t) = \xi_n \sum_{q=1}^{L} \sin(q\omega_o t - \Phi_{nq})$.

The proposed multi-stream receiver structure based on an SSB TMA is shown in Fig. 5. Let us consider that a signal $s(t) \in \mathbb{R}$ at ω_c impinges on the TMA. For the sake of simplicity, we will work with its complex-valued representation $\tilde{s}(t) = u(t)\mathrm{e}^{j\omega_c t} \in \mathbb{C}$, being $u(t) \in \mathbb{C}$ the equivalent baseband signal of $s(t)$, i.e., $s(t) = \Re\{\tilde{s(t)}\}$. According to [7] and Fig. 5, the corresponding signal at the output of the TMA is

$$\tilde{s}^{\mathrm{TMA}}(t,\theta) = u(t)\mathrm{e}^{j\omega_c t} \sum_{n=0}^{N-1} (r_n^{\cos}(t) + j r_n^{\sin}(t))\mathrm{e}^{jkz_n \cos\theta}, \quad (1)$$

whose Fourier transform –after immediate calculations with the simple Fourier transforms of $r_n^{\cos}(t)$ and $r_n^{\sin}(t)$, where the $\delta(\omega + q\omega_o)$ terms are canceled out– is

$$\tilde{S}^{\mathrm{TMA}}(\omega,\theta) = \tfrac{U(\omega-\omega_c)}{2\pi} * \sum_{n=0}^{N-1} \sum_{q=1}^{L} \xi_n \delta(\omega - q\omega_o)\mathrm{e}^{-j\Phi_{nq}}\mathrm{e}^{jkz_n\cos\theta}, \quad (2)$$

with "$*$" being the convolution operator. Turning back to the time domain through the inverse Fourier transform we have

$$\begin{aligned}\tilde{s}^{\mathrm{TMA}}(t,\theta) &= 2u(t) \sum_{q=1}^{L} \sum_{n=0}^{N-1} \xi_n \mathrm{e}^{-j\Phi_{nq}} \mathrm{e}^{jkz_n\cos\theta} \mathrm{e}^{j\omega_q t} \\ &= 2u(t) \sum_{q=1}^{L} \mathrm{e}^{j\omega_q t} \sum_{n=0}^{N-1} I_{nq}^{\mathrm{TMA}} \mathrm{e}^{jkz_n\cos\theta} \\ &= 2u(t) \sum_{q=1}^{L} F_q^{\mathrm{TMA}}(\theta,t) = 2u(t) F^{\mathrm{TMA}}(\theta,t), \quad (3)\end{aligned}$$

where it is demonstrated that $I_{nq}^{\mathrm{TMA}} = \xi_n \mathrm{e}^{-j\Phi_{nq}}$ which corresponds exactly to the target distribution of Fig. 3.

IV. Simulated Example: A Brief Comparison

In this example we take as a reference the radiation pattern in [2, Fig. 11], synthesized with a TMA with switches of $N = 20$ elements and $z_n = \lambda/2$, which performs BF exploiting the beams $q = \{0, 1, 2\}$ corresponding to patterns A, B, and C in Fig. 6. Notice that specular beams at $q = \{-1, -2\}$ (not shown in [2] but introduced in Fig. 6 as patterns B' and C') are spontaneously generated. The corresponding pulse sequences (see [2, Fig. 11(c)]) applied to the static uniform excitations, are obtained through a Particle Swarm Optimization (PSO) algorithm. In this TMA structure, the beam $q = 0$ has no steering capacity and the theoretical antenna efficiency (note that the hardware efficiency [1] is not considered because it depends on the specific selected devices) is calculated as the quotient between the useful and the total mean received powers: $\eta(L) = P_U^{\mathrm{TMA}}/P_R^{\mathrm{TMA}} = \sum_{q=0}^{L-1} p_q / \sum_{q=-\infty}^{\infty} p_q$, where p_q is the mean received power over the harmonic q [1]. Note that $1 - \eta(L)$ corresponds to the power percentage wasted by the unexploited harmonics. In this example $\eta(L = 3) = 30.78\,\%$.

The same pattern can be obtained using identical SWC pulses whose cosine weights [3] are $a_{n2} = a_{n1} = 2a_{n0} = 1/5$ and with ξ_n corresponding to a normalized Gaussian pattern with a standard deviation of $2/3$, leading to $\eta(L = 3) = 88.30\,\%$. We can synthesize the useful beams A, B, and C (see Fig. 6) over the harmonics $q = \{1, 2, 3\}$ with the proposed SSB TMA, using the same ξ_n as for the SWC case, yielding $\eta(L = 3) = 100.00\,\%$ and allowing for steering capacity for all the involved beams. Finally, we quantify the directivity of pattern A for the three approaches, i.e., switches, SWC pulses, and the proposed method, arriving at 2.76 dBi, 11.58 dBi, and 13.82 dBi, respectively.

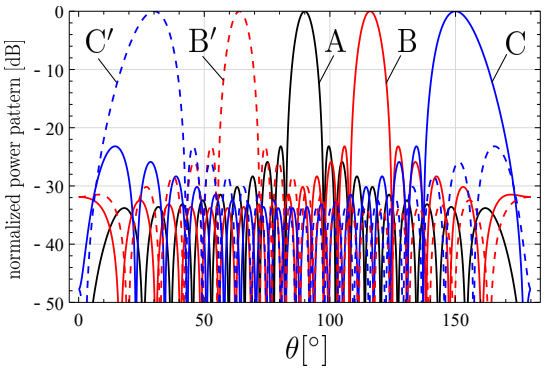

Fig. 6. Beams A, B, C, B', and C' are synthesized both with a TMA with switches and a TMA with SWC pulses over the harmonics $q = \{0, 1, 2, -1, -2\}$. The proposed SSB TMA only generates the useful beams A, B, C over the harmonics $q = \{1, 2, 3\}$.

V. Conclusions

We have proposed a novel strategy for multiple-beam harmonic BF design with TMAs based on the preprocessing of rectangular pulses with the following features: (1) exclusive use of time parameters (agility), (2) independent scanning of the harmonic beams (flexibility), (3) SSB behavior leading to an improved directivity as well as steering ability of all the working beams (efficiency), and (4) time-linear control of the magnitudes of the dynamic excitations without using synthesis optimization algorithms (simplicity).

References

[1] R. Maneiro Catoria, J. Brégains, J. A. Garcia-Naya, L. Castedo, P. Rocca, and L. Poli, "Performance analysis of time-modulated arrays for the angle diversity reception of digital linear modulated signals," *IEEE J. Sel. Topics Signal Process.*, vol. 11, no. 2, pp. 247–258, Mar. 2017.

[2] P. Rocca, Q. Zhu, E. Bekele, S. Yang, and A. Massa, "4-D arrays as enabling technology for cognitive radio systems," *IEEE Trans. Antennas Propag.*, vol. 62, no. 3, pp. 1102–1116, March 2014.

[3] R. Maneiro Catoria, J. Brégains, J. A. Garcia-Naya, and L. Castedo, "Enhanced time-modulated arrays for harmonic beamforming," *IEEE J. Sel. Topics Signal Process.*, vol. 11, no. 2, pp. 259–270, Mar. 2017.

[4] A. M. Yao, W. Wu, and D. G. Fang, "Single-sideband time-modulated phased array," *IEEE Trans. Antennas Propag.*, vol. 63, no. 5, pp. 1957–1968, May 2015.

[5] C. He, A. Cao, X. Liang, R. Jin, and J. Geng, "Beamforming method with periodical amplitude modulation array," in *IEEE Antennas and Propag. Society International Symposium (APSURSI)*, Jul. 2013, pp. 874–875.

[6] S.-C. Pei and C.-C. Tseng, "An efficient design of a variable fractional delay filter using a first-order differentiator," *IEEE Signal Process. Lett.*, vol. 10, no. 10, pp. 307–310, Oct 2003.

[7] R. Maneiro-Catoira, J. C. Brégains, J. A. García-Naya, and L. Castedo, "On the feasibility of time-modulated arrays for digital linear modulations: A theoretical analysis," *IEEE Trans. Antennas Propag.*, vol. 62, no. 12, pp. 6114–6122, Dec 2014.